1   **Cryo-EM reveals how Hsp90 and FKBP immunophilins co-regulate the Glucocorticoid**

2   **Receptor**

3   Chari M. Noddings[1], Jill L. Johnson[2], and David A. Agard[1†]

4   [1]Department of Biochemistry and Biophysics, University of California, San Francisco, San

5   Francisco, CA 94143, USA

6   [2]Department of Biological Sciences, University of Idaho, Moscow, ID 83844, USA

7   [†]Correspondence to: agard@msg.ucsf.edu

8

9   **Abstract**

10   **Hsp90 is an essential molecular chaperone responsible for the folding and activation of**

11   **hundreds of 'client' proteins, including the glucocorticoid receptor (GR)[1-3]. Previously, we**

12   **revealed that GR ligand binding activity is inhibited by Hsp70 and restored by Hsp90,**

13   **aided by co-chaperones[4]. We then presented cryo-EM structures mechanistically detailing**

14   **how Hsp70 and Hsp90 remodel the conformation of GR to regulate ligand binding[5,6]. *In***

15   ***vivo*, GR-chaperone complexes are found associated with numerous Hsp90 co-chaperones,**

16   **but the most enigmatic have been the immunophilins FKBP51 and FKBP52, which further**

17   **regulate the activity of GR and other steroid receptors[7-9]. A molecular understanding of**

18   **how FKBP51 and FKBP52 integrate with the GR chaperone cycle to differentially regulate**

19   **GR activation *in vivo* is lacking due to difficulties reconstituting these interactions. Here,**

20   **we present a 3.01 Å cryo-EM structure of the GR:Hsp90:FKBP52 complex, revealing , for**

21   **the first time, that FKBP52 directly binds to the folded, ligand-bound GR using three novel**

22   **interfaces, each of which we demonstrate are critical for FKBP52-dependent potentiation**

23   **of GR activity *in vivo*. In addition, we present a 3.23 Å cryo-EM structure of the**

24 **GR:Hsp90:FKBP51 complex, which, surprisingly, largely mimics the GR:Hsp90:FKBP52**

25 **structure. In both structures, FKBP51 and FKBP52 directly engage the folded GR and**

26 **unexpectedly facilitate release of p23 through an allosteric mechanism. We also reveal that**

27 **FKBP52, but not FKBP51, potentiates GR ligand binding *in vitro*, in a manner dependent**

28 **on FKBP52-specific interactions. Altogether, we reveal how FKBP51 and FKBP52**

29 **integrate into the GR chaperone cycle to advance GR to the next stage of maturation and**

30 **how FKBP51 and FKBP52 compete for GR:Hsp90 binding, leading to functional**

31 **antagonism.**

32

33 **Introduction**

34   Hsp90 is required for the functional maturation of 10% of the eukaryotic proteome[10].

35 Hsp90 'clients' are enriched in signaling proteins and transcription factors, such as steroid

36 hormone receptors (SHRs), making Hsp90 an important clinical target[1]. SHRs, which include

37 GR, are hormone-regulated transcription factors that depend on Hsp90 for function throughout

38 their lifetimes[7,11-15]. We previously established *in vitro* reconstitution of the 'GR-chaperone

39 cycle', revealing that GR depends on Hsp90 for function due to constant inactivation of ligand

40 binding by Hsp70 and subsequent reactivation by Hsp90[4]. In the GR-chaperone cycle, now

41 understood in atomic detail through cryo-EM, GR ligand binding is regulated by a cycle of three

42 distinct chaperone complexes[5,6]. In this chaperone cycle, GR is first inhibited by Hsp70 and

43 Hsp40, then loaded onto Hsp90:Hop (Hsp70/Hsp90 organizing protein co-chaperone) forming an

44 inactive 'GR-loading complex' (GR:Hsp70:Hsp90:Hop)[5]. Upon ATP hydrolysis by Hsp90, two

45 Hsp70s and Hop are released, and p23 is incorporated to form an active 'GR-maturation

46 complex' (GR:Hsp90:p23), restoring GR ligand binding with enhanced affinity[6]. The cryo-EM

47   structures of the GR-loading complex and GR-maturation complex reveal Hsp70 and Hsp90

48   locally unfold and refold the GR LBD in a controlled manner to directly regulate ligand binding.

49   *In vivo*, additional Hsp90 co-chaperones are found associated with the GR-chaperone

50   cycle, including the large immunophilins, FKBP51 and FKBP52[7]. FKBP51 and FKBP52 are

51   peptidyl proline isomerases (PPIases) that contain an N-terminal FK1 domain with PPIase

52   activity, an FK2 domain lacking PPIase activity, and a C-terminal TPR domain, which

53   canonically binds the EEVD motifs at the C-termini of Hsp90 and Hsp70[16-19]. Additionally, the

54   TPR domain contains a helical extension at the C-terminus (Helix 7e), which was previously

55   described to bind the C-terminal domain (CTD) closed dimer interface of Hsp90[20,21]. Although

56   FKBP51 and FKBP52 are 70% similar in sequence, these co-chaperones have antagonistic

57   functional effects on GR *in vivo*[8]. FKBP51 inhibits GR ligand binding, nuclear translocation, and

58   transcriptional activity, while FKBP52 potentiates each of these fundamental GR activities[22-32].

59   FKBP51 and FKBP52 have also been implicated in the regulation of all other SHRs[8,9]. Due to

60   the critical importance of steroid hormone signaling in the cell, altered expression of FKBP51

61   and FKBP52 is associated with various endocrine-related disease states, including a wide variety

62   of cancers, infertility, stress and anxiety disorders, and immune-related diseases[8,9,33]. Despite

63   their importance, the absence of structures of FKBP co-chaperones bound to Hsp90:client

64   complexes precludes a mechanistic understanding of how these co-chaperones integrate with

65   Hsp90:client complexes to regulate client function or how to design selective small-molecule

66   therapeutics[33-38]. Here we present a 3.01 Å cryo-EM structure of the GR:Hsp90:FKBP52

67   complex, revealing for the first time how FKBP52 integrates into the GR-chaperone cycle and

68   directly binds to the active client, potentiating GR activity *in vitro* and *in vivo*. We also present a

69   3.23 Å cryo-EM structure of the GR:Hsp90:FKBP51 complex, revealing how FKBP51 competes

70   with FKBP52 for GR:Hsp90 binding and demonstrating how FKBP51 can act a potent

71   antagonist to FKBP52.

72

73   **Results**

74   *GR:Hsp90:FKBP52 Structure Determination*

75   The GR:Hsp90:FKBP52 complex was prepared by *in vitro* reconstitution of the complete

76   GR-chaperone cycle. GR DBD-LBD (amino acids 418-777) (hereafter, GR for simplicity) with

77   an N-terminal maltose-binding protein (MBP) tag was incubated with Hsp70, Hsp40, Hop,

78   Hsp90, p23, and FKBP52, allowing GR to progress through the chaperone cycle to reach the

79   GR:Hsp90:FKBP52 complex (Extended Data Fig. 1a,b). The complex was stabilized with

80   sodium molybdate and then purified by affinity purification on MBP-GR followed by size

81   exclusion chromatography and light crosslinking (Extended Data Fig. 1c,d). A 3.01 Å cryo-EM

82   reconstruction of the GR:Hsp90:FKBP52 complex was obtained using RELION and CryoSparc,

83   with atomic models built using Rosetta (Fig. 1a,b; Extended Data Fig. 1e, 2). The structure

84   revealed a fully closed, nucleotide bound Hsp90 dimer (Hsp90A and Hsp90B) complexed with a

85   single GR and a single FKBP52, which occupied the same side of Hsp90 (Fig. 1a,b, ED. Fig. 3a).

86   Despite using a multi-domain GR construct, only the GR LBD was visible in the density map.

87

88   *Hsp90 Stabilizes the GR LBD in a Folded, Ligand-Bound State*

89   In the GR:Hsp90:FKBP52 complex, GR adopts a fully folded, ligand-bound

90   conformation (Extended Data Fig. 3b) distinct from that adopted in the GR:Hsp90:p23

91   maturation complex (discussed below). The folded GR is stabilized by Hsp90 at three major

92   interfaces (Fig. 1c-e, Extended Data Fig. 3c-f): (1) Hsp90 Src loop:GR hydrophobic patch, (2)

93   Hsp90 MD/CTD:GR Helix 1, and (3) Hsp90 lumen:GR pre-helix 1. In the first interface, the

94   Hsp90A Src loop (Hsp90$^{345\text{-}360)}$, flips out from the Hsp90 lumen, to interact with the previously

95   described hydrophobic patch formed by GR Helices 9/10 and the GR C-terminus[6]

96   (approximately 767 Å^2 of buried surface area (BSA)) (Fig. 1c, Extended Data Fig. 3c). Along the

97   Src loop, Hsp90A ^{F349,L351,F352,E353} contact GR helices 9/10 and the conserved, solvent exposed

98   Hsp90A^{W320} interacts with GR^{F774} on the GR C terminus. Notably, Hsp90A^{W320,F349} also make

99   contact with GR in the GR-loading complex and GR-maturation complex, although at quite

100   different locations[5,6]. Additionally, there are multiple hydrogen bonds formed between the Hsp90

101   NTD/MD to GR Helix 10 and the GR C-terminus (GR^{K777}).

102   Interface 2 is comprised of Hsp90^{Y604} packing against GR Helix 1 (GR$^{532\text{-}539}$) and

103   Hsp90^{Y627} sticking into a hydrophobic pocket on GR formed by Helices 3, 4, and 9

104   (approximately 345 Å^2 BSA) (Fig. 1d, Extended Data Fig. 3d,e). This GR hydrophobic pocket

105   was previously identified in the androgen receptor (AR) as a druggable hydrophobic site (BF3)[39].

106   In interface 3, the unstructured GR pre-helix 1 region (GR$^{519\text{-}531}$) is threaded through the closed

107   Hsp90 lumen (approximately 758 Å^2 BSA)(Fig. 1e, Extended Data Fig. 3f). Two hydrophobic

108   residues on GR (GR^{P522,P526}) occupy two hydrophobic pockets within the Hsp90 lumen. The

109   interaction is further stabilized by multiple polar and hydrophobic interactions between GR pre-

110   helix 1 and the Hsp90A/B amphipathic helical hairpin (Hsp90$^{606\text{-}628}$) and Hsp90 MD.

111

112   *FKBP52 Interacts with the Closed Hsp90*

113   FKBP52 engages the closed Hsp90 at three major interfaces (Fig. 1f,g, Extended Data

114   Fig. 4a-c): (1) FKBP52 TPR H7e:Hsp90A/B CTDs, (2) FKBP52 TPR:Hsp90B MEEVD, and (3)

115   FKBP52 TPR:Hsp90B CTD. In Interface 1, the extended TPR C-terminal H7e (FKBP52$^{387\text{-}424}$)

116   binds in a hydrophobic cleft formed by the Hsp90A/B CTDs at the closed dimer interface

117   (approximately 1109 $Å^2$ BSA)(Fig. 1f, Extended Data Fig. 4a). As compared to the crystal

118   structure, H7e breaks at positions FKBP52$^{411-414}$ to allow hydrophobic residues

119   (FKBP52^{L410,Y411,M414,F415,L418}) to flip into the hydrophobic cleft formed by the Hsp90 CTDs,

120   consistent with the FKBP51 H7e:Hsp90 interaction observed by cryo-EM[20]. Mutating the

121   corresponding conserved residues on FKBP51 H7e (FKBP51^{M412,F413} corresponding to FKBP52

122   ^{M414,F415}) abolishes FKBP51:Hsp90 binding, indicating the importance of this binding site[20]. The

123   interface is further stabilized by multiple hydrogen bonds and salt bridges from Hsp90A/B to

124   H7e flanking the helix break (Extended Data Fig. 4a). Furthermore, a portion of the Hsp90B

125   MEEVD linker (Hsp90B$^{700-706}$) binds along FKBP52 H7e (Extended Data Fig. 4a).

126   In Interface 2, the C-terminal MEEVD peptide motif of Hsp90B binds in the FKBP52

127   TPR helical bundle (approximately 779 $Å^2$ BSA) (Fig. 1g, Extended Data Fig. 4b), with multiple

128   hydrogen bonds, salt bridges, and hydrophobic interactions, analogous to FKBP51:Hsp90^{MEEVD}

129   structures[19,20]. However, the MEEVD peptide binds in an opposite orientation relative to the

130   FKBP52:Hsp90^{MEEVD} crystal structure[18], which may have been incorrectly modeled as

131   previously suggested[19,40]. Interface 3 is comprised of the FKBP52 TPR helices 5/6 binding to the

132   Hsp90B CTD, stabilized by multiple hydrogen bonds (approximately 193 $Å^2$ BSA) (Extended

133   Data Fig. 4c), also observed in the FKBP51:Hsp90 cryo-EM structure[20]. While the interactions

134   between FKBP52 TPR/H7e:Hsp90 are conserved in the FKBP51:Hsp90 structure, the positions

135   of the FKBP52 FK1 and FK2 domains are significantly altered (Extended Data Fig. 4d), owing

136   to the presence of the bound GR client, as discussed below.

137

138   *FKBP52 Directly Interacts with GR, which is Functionally Important In Vivo*

139   Unexpectedly, FKBP52 directly and extensively interacts with GR, with all three

140   FKBP52 domains wrapping around GR, cradling the folded, ligand-bound receptor near the GR

141   ligand-binding pocket (Fig. 2a). The tertiary structure within each FKBP52 domain closely

142   matches isolated domains from FKBP52 crystal structures; however, the interdomain angles are

143   significantly different (Extended Data Fig. 4d), likely owing to the extensive interaction with

144   GR. There are three major interfaces between FKBP52 and GR (Fig. 2b-d): (1) FKBP52

145   FK1:GR, (2) FKBP52 FK2:GR, and (3) FKBP52 FK2-TPR linker:GR Helix 12.

146   In interface 1, FKBP52 FK1 interacts with a large surface on GR, canonically used for

147   GR dimer formation, consisting of the GR post-helix 1 strand (helix 1-3 loop), helix 5, and β1,2

148   (approximately 280 Å^2 BSA) (Fig. 2b). 3D variability analysis in CryoSparc reveals that the

149   interaction between FKBP52 FK1 and GR is highly dynamic, even as the other FKBP52

150   domains (FK2, TPR) remain stably associated with GR (Supplemental Movies 1-2). At the

151   FK1:GR interface, GR^{Y545} on the post-Helix 1 strand interacts with a hydrophobic surface

152   formed by the FKBP52$^{81-88}$ loop and forms a hydrogen bond with FKBP52^{Y113}. Supporting this

153   interaction, residues in the GR post-helix 1 strand (GR$^{544-546}$) have previously been implicated in

154   FKBP51/52-dependent regulation of GR activity[41,42].

155   In addition, the FKBP52 proline-rich loop (β4-β5 loop or 80S loop) contacts GR Helix 5

156   and β1,2. 3D variability analysis in CryoSparc reveals that the proline-rich loop positioning is

157   flexible, deviating from the position in the crystal structure (PDB ID: 4LAV)[43] and adopting

158   different interfaces with GR (Supplemental Movies 3-4). In the consensus 3D refinement map,

159   the proline-rich loop adopts a position similar to the crystal structure, and FKBP52^{A116,S118,P119}

160   interact with the tip of GR Helix 5 and β1,2. The FKBP52^{P119L} mutation has been shown to

161   reduce GR and AR activation *in vivo*, while FKBP52^{A116V} has been shown to increase AR

162   activation *in vivo*[29]. We also demonstrate that the FKBP52[S118A] mutation significantly reduces

163   FKBP52-dependent GR potentiation *in vivo* (Fig. 2e), further demonstrating the functional

164   significance of this interaction site. In addition, S118 has been identified as a phosphorylation

165   site on FKBP52, but not FKBP51 (qPTM database[44]) (possibly due to the unique adjacent

166   proline on FKBP52 (P119) which could act as a signal for proline-directed protein kinases).

167   Phosphorylation at FKBP52 [S118] may help promote the interaction between the proline-rich loop

168   and GR, which could also explain the large effect of the FKBP52[S118A] mutation *in vivo*.

169   While the FKBP52 FK1 domain is known to have PPIase enzymatic activity, GR is not

170   bound in the PPIase active site and accordingly, no GR prolines were found to have been

171   isomerized compared to other GR structures (PDB ID: 1M2Z[45], 7KRJ[6]). Consistent with this,

172   mutation of GR prolines does not disrupt FKBP52-dependent regulation of GR[42]. Additionally,

173   mutations that disrupt PPIase activity do not affect FKBP52-dependent GR potentiation *in vivo*[29].

174   Conversely, PPIase inhibitors have been shown to block the FKBP52-dependent potentiation of

175   GR *in vivo*[23]. This can now be understood, as docking of PPIase inhibitors (FK506, rapamycin)

176   into the PPIase active site demonstrate that the inhibitors would sterically block the FKBP52

177   FK1:GR interface (Extended Data Fig. 4e), which was previously hypothesized[23,29].

178   Interface 2 is comprised of the FKBP52 FK2[Y161] sticking into a shallow hydrophobic

179   pocket formed by GR Helix 3 and the Helix 11-12 loop (GR[T561, M565,E748]) and a hydrogen bond

180   between the FKBP52 backbone and GR[E748] (approximately 125 Å^2 BSA) (Fig. 2c). Supporting

181   this interaction, we show that the FKBP52[Y161D] mutation significantly reduces FKBP52-

182   dependent GR potentiation *in vivo*, demonstrating the importance of this interaction (Fig. 2e). In

183   interface 3, the solvent exposed, conserved W259 on the FKBP52 FK2-TPR linker makes

184   electrostatic and hydrophobic interactions with GR Helix 12 (approximately 235 Å^2 BSA) (Fig.

185   2d), which adopts the canonical agonist-bound position even in the absence of a stabilizing

186   coactivator peptide interaction[45] (Extended Data Fig. 3b). We show that the corresponding

187   FKBP52[W259D] mutation significantly reduces FKBP52-dependent GR potentiation *in vivo*,

188   demonstrating the functional importance of this single residue (Fig. 2e). Interestingly,

189   FKBP52[W259] is also conserved in the FKBP-like co-chaperone XAP2 and a recent structure

190   reveals XAP2 engages with an Hsp90-client using the analogous XAP2[W168], suggesting this

191   residue is critical more broadly for FKBP cochaperone:client engagement[46]. At interface 3,

192   FKBP52[K254,E257,Y302,Y303] make further polar interactions between the FK2-TPR linker and GR

193   Helix 12 (Fig. 2d). While a significant portion of the GR Helix 12 co-activator binding site is

194   available in the FKBP52-bound GR, the N-terminus of a co-activator peptide would sterically

195   clash with the FKBP52 TPR based on the GR:co-activator peptide structure[45] (Extended Data

196   Fig. 5b). Thus, coactivator binding in the nucleus could help release GR from its complex with

197   Hsp90:FKBP52. We also find that the residues at the FKBP52:GR interfaces are conserved

198   across metazoans (Fig. 2f,g), in agreement with our results that single point mutations at each of

199   the three FKBP52:GR interfaces has a significant effect on GR function *in vivo*.

200

201   *FKBP52 Advances GR to the Next Stage of Maturation*

202   We previously described another GR-chaperone complex, the GR-maturation complex

203   (GR:Hsp90:p23)[6], which has important similarities and differences when compared to the

204   GR:Hsp90:FKBP52 complex. Both the GR-maturation complex and the GR:Hsp90:FKBP52

205   complex are comprised of a closed Hsp90 dimer and a folded, ligand-bound GR (Fig. 3a). In the

206   GR:Hsp90:FKBP52 complex, GR is rotated by approximately 45° relative to the GR-maturation

207   complex (Fig. 3a). The Hsp90A Src loop interacts with the GR pre-Helix 1 strand in the

208 maturation complex, but flips out to stabilize the rotated GR position in the GR:Hsp90:FKBP52

209 complex, by interacting with the GR hydrophobic patch (GR Helices 9/10)(Fig. 3b,c). In both

210 complexes, the pre-Helix 1 strand of GR is threaded through the Hsp90 lumen; however, in the

211 GR:Hsp90:FKBP52 complex, GR has translocated through the Hsp90 lumen by two residues,

212 positioning two prolines ($GR^{P522,P526}$) in the hydrophobic pockets in the Hsp90 lumen rather than

213 two leucines ($GR^{L525,L528}$) (Fig. 3d). This translocation positions the GR LBD further from

214 Hsp90, likely allowing enough space for the observed GR rotation. The rotation of GR may also

215 facilitate GR LBD dimerization, which is on pathway to activation (Extended Data Fig. 5c).

216 Despite the translocation and rotation of GR, Hsp90 uses the same surfaces to bind GR (Hsp90B

217 amphipathic helical hairpin, Hsp90A Src loop, $Hsp90A^{W320}$); however, the GR contact surfaces

218 are different.

219

220 *FKBP52 Competes with p23 for GR:Hsp90 Binding through Allostery*

221   Surprisingly, FKBP52 competes with p23 to bind the GR:Hsp90 complex, although there

222 is no direct steric conflict between FKBP52 and p23 binding (Fig. 3a). During 3D classification

223 on the cryo-EM dataset, GR:Hsp90:p23 complexes were observed at low abundance; however,

224 the GR:Hsp90:FKBP52 complexes showed no apparent p23 density (Extended Data Fig. 2),

225 despite p23 being present at high concentration in the reconstitution mix. Furthermore, FKBP52

226 was found only associated with the rotated GR position, while the GR position in the p23-

227 containing classes was only consistent with the GR-maturation complex. Thus, FKBP52 appears

228 to specifically bind the rotated GR position, which is not compatible with p23 binding. This is

229 consistent with mass spectrometry studies, demonstrating FKBP52 competes off p23 to form a

230 stable GR:Hsp90:FKBP52 complex[47]. In the rotated GR position, the Hsp90A Src loop flips out

231   of the Hsp90 lumen to bind the GR hydrophobic patch, which was previously engaged by the

232   p23 tail-helix (Fig. 3a-c). Thus, rotation of GR dictates the accessibility of the hydrophobic patch

233   to either Hsp90 or p23. FKBP52 stabilizes the rotated position of GR and therefore favors Hsp90

234   binding to GR over p23 and this in turn leads to p23 dissociation.

235

236   *FKBP52 Potentiates GR Ligand Binding In Vitro*

237   To quantitatively assess the functional significance of FKBP52 on GR activation, we

238   added FKBP52 to the *in vitro* reconstituted GR-chaperone cycle, using the GR DBD-LBD

239   construct (residues 418-777) and monitored GR ligand binding, as previously described[4,6].

240   Addition of FKBP52 to the GR chaperone cycle resulted in the enhancement of GR ligand

241   binding above the already enhanced GR + chaperones control reaction at equilibrium (Fig. 3e),

242   strongly suggesting FKBP52 potentiates the GR ligand binding affinity beyond the minimal

243   chaperone mixture, consistent with reports *in vivo*[23]. We hypothesized that FKBP52 functions in

244   a similar manner to the p23 tail-helix in stabilizing the ligand-bound GR. As previously

245   described, removal of the p23 tail-helix (p23Δhelix) resulted in a decrease in GR ligand binding

246   activity in the GR-chaperone system[6]; however, addition of FKBP52 to the reaction fully rescued

247   GR ligand binding in the p23Δhelix background (Fig. 3e), suggesting FKBP52 functions in a

248   similar manner to the p23 tail-helix in stabilizing the ligand-bound GR. Additionally, in the

249   p23Δhelix background, FKBP52 potentiated ligand binding to a greater extent than in the

250   wildtype p23 background. We hypothesize that removing the p23 tail-helix alleviates the

251   competition between p23 and FKBP52, allowing p23 to remain bound to the GR:Hsp90:FKBP52

252   complex. Given that p23 is known to stabilize the closed Hsp90 conformation[6,48], the enhanced

253   ligand binding in the p23Δhelix background may be due to stabilization of closed Hsp90 by p23.

254   Interestingly, FKBP52 also affected GR ligand binding independent of Hsp90, with addition of

255   FKBP52 to GR resulting in enhanced ligand binding, likely due to an Hsp90-independent

256   chaperoning effect[16,49] (Extended Data Fig. 5d).

257

258   *FKBP52 Functionally Replaces p23 In Vitro when Hsp90 Closure is Stabilized*

259   Given that FKBP52 can functionally replace the p23 tail-helix, we wondered whether

260   FKBP52 could also functionally replace p23 altogether. p23 is known to stabilize Hsp90 NTD

261   closure through the globular p23 domain[6,48] in addition to stabilizing the ligand-bound GR

262   through the p23 tail-helix. Omitting p23 from the GR-chaperone cycle drastically reduces GR

263   ligand binding, as previously described[4,6]. The addition of FKBP52 in place of p23 results in a

264   modest increase in ligand binding but does not fully rescue ligand binding activity (Fig. 3f). We

265   reasoned this could be due to the inability of FKBP52 to sufficiently stabilize Hsp90 closure, as

266   previously suggested[50]. Therefore, we added molybdate to these reactions, which stabilizes NTD

267   closure by acting as a γ-phosphate analogue in the Hsp90 NTD ATP-binding site[6,51]. Addition of

268   molybdate to the reaction lacking p23 resulted in a small increase in GR ligand binding but did

269   not fully rescue ligand binding activity. However, addition of molybdate to the reactions

270   containing FKBP52 without p23 resulted in a full reactivation of ligand binding and even

271   potentiated ligand binding over the control GR + chaperones reaction (Fig. 3f), much like with

272   p23Δhelix. Thus, FKBP52 is able to functionally replace p23 if Hsp90 NTD closure is stabilized.

273   Taken together, these results suggest FKBP52 can stabilize the ligand-bound GR, like p23, but

274   cannot stabilize the closed Hsp90 NTD conformation, which requires p23.

275

276   *GR:Hsp90:FKBP51 Structure Determination*

277   *In vivo* the interplay between FKBP52 and the highly similar FKBP51 have profound

278   implications for GR activity. FKBP51 is functionally antagonistic to FKBP52-dependent

279   potentiation of GR *in vivo,* thus the relative ratios of FKBP51 and FKBP52 dictate GR activity

280   levels[23,28,52]. In order to understand mechanistically how FKBP51 antagonizes FKBP52, we

281   prepared the analogous GR:Hsp90:FKBP51 complex (Extended Data Fig. 1c-e). We obtained a

282   3.23 Å cryo-EM reconstruction of GR:Hsp90:FKBP51 using RELION and CryoSparc, with

283   atomic models built using Rosetta (Fig. 4a,b, Extended Data Fig. 6). Contrary to our

284   expectations, the FKBP51-containing structure appears nearly identical to the FKBP52-

285   containing structure. The GR:Hsp90:FKBP51 structure reveals a fully closed, nucleotide bound

286   Hsp90 dimer complexed with a single GR and a single FKBP51, which occupy the same side of

287   Hsp90 (Fig. 4a,b, Extended Data Fig. 7a). The FKBP51:Hsp90 interactions are analogous to the

288   FKBP52:Hsp90 interactions, including the Hsp90B MEEVD:TPR interface and the Hsp90

289   CTD:TPR Helix 7e interface, also seen in the Hsp90:FKBP51:p23 structure[20] (Fig. 4b, Extended

290   Data Fig. 7b-d). The GR:Hsp90 interfaces are nearly identical when comparing the FKBP51 and

291   FKBP52-containing complexes, including the Hsp90 Src loop:GR hydrophobic patch interface

292   and the Hsp90 lumen:GR pre-Helix 1 strand interface (Fig. 4b, Extended Data Fig. 7e-g).

293   FKBP51 also directly binds GR in an analogous manner to FKBP52 (Fig. 4c-e). FKBP51

294   binds the folded, ligand-bound, rotated GR using the same three major interfaces (1) FKBP51

295   FK1:GR, (2) FKBP51 FK2:GR Helix 3, and (3) FKBP51 FK2-TPR linker:GR Helix 12. The

296   GR:FKBP52 interaction residues are largely conserved for GR:FKBP51 (Fig. 2f). As with the

297   FKBP52-containing structure, no GR prolines appear to be isomerized and the PPIase inhibitors

298   rapamycin and FK506 sterically clash with the GR backbone. Interestingly, the small FKBP51-

299   specific inhibitor, SAFit2 (PDB ID: 6TXX)[34,53], does not clash with the GR backbone and may

300   be accommodated in this complex with only side chain rotations, consistent with *in vivo* data

301   from Baischew et al. 2022 (Extended Data Fig. 7h). Furthermore, the FKBP51 FK1 domain and

302   FK1 proline-rich loop are highly dynamic, as revealed by CryoSparc 3D variability analysis,

303   analogous to the FKBP52-containing structure (Supplemental Movies 5-6). However, in the

304   GR:Hsp90:FKBP51 consensus map and corresponding atomic model, the FK1 domain contacts

305   GR at a different angle relative to the GR:Hsp90:FKBP52 model; thus, the FK1:GR interface is

306   distinct between the two complexes, specifically at the functionally important, but divergent,

307   residue 119 in the proline-rich loop (FKBP51^{L119}, FKBP52^{P119}) (Fig. 2b, 3c)[29], which we

308   investigated further below.

309

310   *Functional Difference Between FKBP51 and FKBP52 Depends on Residue 119*

311   To quantitatively assess the functional effect of FKBP51 on GR *in vitro*, we added

312   FKBP51 to the GR-chaperone cycle and measured ligand binding activity. FKBP51 had no effect

313   on the GR equilibrium value, unlike FKBP52, which potentiates GR ligand binding (Extended

314   Data Fig. 8a). However, we found FKBP51 can functionally replace the p23 tail-helix or p23 (if

315   molybdate is added), just as we observed with FKBP52 (Fig. 4f, Extended Data Fig. 8b).

316   However, FKBP51 does not potentiate GR ligand binding in any of these conditions, unlike

317   FKBP52, recapitulating *in vivo* findings.

318   The residues responsible for the functional difference between FKBP51 and FKBP52 *in*

319   *vivo* have been suggested to come from the proline-rich loop on the FK1 domain, specifically the

320   divergent residue 119 (FKBP51^{L119}, FKBP52^{P119})[29]. To assess whether this residue is responsible

321   for the functional difference between FKBP51 and FKBP52 *in vitro*, we swapped residue 119 in

322   FKBP51 and FKBP52 and added these mutants (FKBP51 L119P, FKBP52 P119L) to the *in vitro*

323   reconstituted GR-chaperone cycle. We then measured ligand binding activity in the p23Δhelix

324   background, where the largest potentiation due to FKBP52 is observed. Surprisingly, the residue

325   119 swapped mutants almost fully reversed the effects of FKBP51 and FKBP52 on GR—

326   FKBP51 L119P potentiated GR ligand binding over the GR + chaperones control reaction, while

327   FKBP52 P119L showed significantly less potentiation of ligand binding compared to wildtype

328   FKBP52 (Fig. 4f). These results are consistent with the effects of the FKBP51/52 residue 119

329   swapped mutants *in vivo*[29]. Thus, residue 119 on the proline-rich loop provides a critical

330   functional difference between the activities of FKBP51 and FKBP52 toward GR *in vitro* and *in*

331   *vivo*, likely driven via the differential positioning of the loop seen in our consensus structures.

332

333   **Discussion**

334   We present the first structures of the FKBP51 and FKBP52 co-chaperones bound to an

335   Hsp90-client complex. The 3.01 Å GR:Hsp90:FKBP52 structure reveals that FKBP52 directly

336   and extensively binds the client using three novel interfaces that stabilize the folded, ligand-

337   bound conformation of GR. We show for the first time, that FKBP52 enhances GR ligand

338   binding *in vitro*, consistent with *in vivo* reports, and that each of the three observed GR:FKBP52

339   interfaces is critical for FKBP52-dependent potentiation *in vivo*. We also provide a 3.23 Å

340   GR:Hsp90:FKBP51 structure, unexpectedly demonstrating FKBP51 binds to the GR:Hsp90

341   complex in a similar manner to FKBP52. The FKBP51 interaction with closed Hsp90 is distinct

342   from a previous NMR model[54], but consistent with a recent cryo-EM structure demonstrating

343   FKBP51 binds closed Hsp90[20]. Thus, these structures provide a molecular explanation for the

344   functional antagonism between these two co-chaperones.

345   A recent study by Baischew et al. 2022 using *in vivo* chemical crosslinking validates our

346   structures remarkably well, recapitulating all three major GR:FKBP51/52 contacts as well as the

347   FKBP-mediated rotated GR position. Given that the *in vivo* crosslinking between GR and

348   FKBP51/52 was performed in the absence of ligand, together our findings demonstrate that

349   FKBP51 and FKBP52 bind the apo GR LBD in a similar, if not nearly identical manner to the

350   ligand-bound GR LBD observed here in our structures. While our high-resolution

351   reconstructions unambiguously contain ligand, apo GR:Hsp90:FKBP51/52 complexes likely

352   exist in our dataset, but are less well-ordered (consistent with the results from the GR-maturation

353   complex structure[6]). Baischew et al. 2022 provides further *in vivo* validation of our structural

354   models by demonstrating FK506 inhibits FKBP51-dependent regulation of GR *in vivo*, while

355   SAFit2 does not (Extended Data Fig. 4e, 7h), and that the FKBP51/52 FK1 domain is

356   dynamically associated with GR relative to the other domains (Supplementary Movies 1-6).

357   Altogether, these studies complement each other extraordinarily well, demonstrating, for the first

358   time, direct association of FKBP51 and FKBP52 with the GR LBD *in vivo* and *in vitro* at single-

359   residue resolution.

360   Surprisingly, our structures also demonstrate that FKBP51 and FKBP52 compete with

361   p23 to bind the GR:Hsp90 complex through an allosteric mechanism. Previous reports showed

362   FKBP51 and p23 could simultaneously bind the closed Hsp90 in the absence of client[20]. We

363   demonstrate that the position of the client can dictate which co-chaperone is bound, with the

364   FKBPs and p23 binding to distinct GR positions. FKBP51 and FKBP52 both stabilize a rotated

365   position of GR relative to the GR-maturation complex. One functional consequence of this

366   rotated position may be to promote GR dimerization, which is a required step in GR activation.

367   The rotated GR position relieves this steric hindrance to dimerization in the GR-maturation

368 complex and would allow the GR LBD to dimerize once FKBP51/52 release (Extended Data

369 Fig. 5c). Indeed, a previous report has suggested FKBP51/52 promote AR dimerization *in* vivo[55],

370 raising the possibility that the FKBPs promote this next step in SHR maturation.

371 Our structures also contribute to an emerging theme in which Hsp90 cochaperones bind

372 to distinct Hsp90 conformations, while simultaneously binding to specific client

373 conformations[5,6,46,51,56]. FKBP51 and FKBP52 each wrap around the folded, ligand-bound client

374 using all three FKBP domains, while the FKBP TPR Helix 7e binds the closed Hsp90

375 conformation. The Helix 7e is found in many TPR-containing co-chaperones[20], however, our

376 structures, along with others, reveal the TPR Helix 7e can bind Hsp90 in distinct positions due to

377 sequence divergence of H7e at the Hsp90 binding site[46,56]. Although the FKBPs directly contact

378 GR, they do not appear to isomerize GR prolines or engage the GR NLS1 (nuclear localization

379 signal 1) ($GR^{467-505}$)[57] to regulate GR activity, as previously hypothesized[13,58-60]

380 While FKBP51 binds similarly to FKBP52, competing with p23 and stabilizing the

381 rotated GR, we find that FKBP51 does not significantly enhance GR ligand binding *in vitro*, like

382 FKBP52, consistent with *in vivo* reports[23 27]. Interestingly, we find residue 119 on FKBP51/52 is

383 critical for enhancement of ligand binding *in vitro*, also consistent with *in vivo* reports[29]. NMR

384 studies have found the proline at residue 119 on FKBP52 decreases dynamics of the proline-rich

385 loop (also called 80S loop or β4-β5 loop) relative to the leucine at FKBP51[61]. Analysis of

386 dynamics of our structures using 3D variability analysis demonstrates that the proline-rich loop

387 is highly dynamic in its interaction with GR. Thus, the dynamics of this loop may dictate the

388 specificity and/or stability of this interaction, leading to distinct regulation of GR activity.

389 Based on our structures of the GR:Hsp90:FKBP51 and GR:Hsp90:FKBP52 complexes,

390 we propose additional steps in the GR-chaperone cycle that account for FKBP51/52

391   incorporation and subsequent regulation of GR activity in the cell (Fig. 5). In the cytosol, GR

392   cycles between Hsp70 and Hsp90, which locally unfold and refold GR to directly control ligand

393   binding, as previously described[4-6]. Once the folded, ligand-bound GR reaches the GR-

394   maturation complex (GR:Hsp90:p23), either FKBP51 or FKBP52 can bind the complex and

395   compete with p23 to advance GR to the next stage of maturation. Given that the folded GR is

396   strongly stabilized and tightly associated with Hsp90 and the FKBPs, we suggest that it is

397   unlikely that ligand binding or unbinding happens in the context of FKBP-bound complexes.

398   Instead, we propose that ligand binds prior to the formation of either the GR-maturation complex

399   or the GR:Hsp90:FKBP complexes, and that unbinding mostly occurs by recycling GR back to

400   Hsp70, as previously described[4-6].

401   After reaching the GR-maturation complex, the functional outcome for GR is dictated by

402   FKBP51 and FKBP52, which compete to bind the GR:Hsp90 complex. FKBP52 stabilizes the

403   ligand-bound GR, resulting in enhanced ligand affinity, and facilitates rapid GR nuclear

404   translocation on dynein[22,24,25,62], allowing GR to proceed with dimerization and activation of

405   transcription in the nucleus. In contrast, FKBP51 binding keeps GR sequestered in the cytosol

406   and recycles GR back to the chaperone cycle, inhibiting GR translocation and transcription

407   activation. Interestingly, the expression of FKBP51, but not FKBP52, is upregulated by GR (as

408   well as PR and AR), leading to a short negative feedback loop, which may help dampen chronic

409   GR activation and signaling[27,63-67]. Thus, the relative concentrations of FKBP51 and FKBP52 in

410   the cell dictate the level of GR activity *in vivo*[23,28,52].

411   Beyond GR, FKBP51/52 are known to regulate the entire SHR class and given the

412   sequence and structural conservation of the SHR LBDs at the FKBP contact sites, we propose

413   FKBP51 and FKBP52 engage with the rest of the SHRs in a similar manner to GR (Extended

414   Data Fig. 9a,b). Thus, FKBP51/52 can fine-tune the activity of these critical and clinically

415   important signaling molecules and allow for crosstalk between the hormone signaling pathways.

416   Altogether, we demonstrate how Hsp90 provides a platform for the FKBP co-chaperones to

417   engage Hsp90 clients after Hsp90-dependent folding and promote the next step of client

418   maturation, providing a critical layer of functional regulation.

419

Acknowledgements

Author Contributions

C.M.N. designed and executed biochemical experiments, cryo-EM sample preparation, data

collection, data processing, and model building. J.L.J. executed yeast *in vivo* assays and

interpreted the results. C.M.N. and D.A.A. conceived the project, interpreted the results, and

wrote the manuscript.

Competing Interests

The authors declare no competing interests.

References

1   Taipale, M., Jarosz, D. F. & Lindquist, S. HSP90 at the hub of protein homeostasis: emerging mechanistic insights. **11**, 515-528, doi:10.1038/nrm2918 (2010).

2   Schopf, F. H., Biebl, M. M. & Buchner, J. The HSP90 chaperone machinery. *Nature Reviews Molecular Cell Biology* **18**, 345-360, doi:10.1038/nrm.2017.20 (2017).

3   Taipale, M. *et al.* Quantitative analysis of HSP90-client interactions reveals principles of substrate recognition. *Cell* **150**, 987-1001, doi:10.1016/j.cell.2012.06.047 (2012).

4   Kirschke, E., Goswami, D., Southworth, D., Griffin, P. & Agard, D. Glucocorticoid Receptor Function Regulated by Coordinated Action of the Hsp90 and Hsp70 Chaperone Cycles. *Cell* **157**, 1685-1697, doi:10.1016/j.cell.2014.04.038 (2014).

5   Wang, R. Y. *et al.* Structure of Hsp90-Hsp70-Hop-GR reveals the Hsp90 client-loading mechanism. *Nature* **601**, 460-464, doi:10.1038/s41586-021-04252-1 (2022).

6   Noddings, C. M., Wang, R. Y., Johnson, J. L. & Agard, D. A. Structure of Hsp90-p23-GR reveals the Hsp90 client-remodelling mechanism. *Nature* **601**, 465-469, doi:10.1038/s41586-021-04236-1 (2022).

7   Pratt, W. B. & Toft, D. O. Steroid Receptor Interactions with Heat Shock Protein and Immunophilin Chaperones. *Endocrine Reviews* **18**, 306-360, doi:10.1210/edrv.18.3.0303 (1997).

8   Storer, C. L., Dickey, C. A., Galigniana, M. D., Rein, T. & Cox, M. B. FKBP51 and FKBP52 in signaling and disease. **22**, 481-490, doi:10.1016/j.tem.2011.08.001 (2011).

9   Zgajnar, N. R. *et al.* Biological Actions of the Hsp90-binding Immunophilins FKBP51 and FKBP52. *Biomolecules* **9**, doi:10.3390/biom9020052 (2019).

10   Zhao, R. *et al.* Navigating the chaperone network: an integrative map of physical and genetic interactions mediated by the hsp90 chaperone. *Cell* **120**, 715-727, doi:10.1016/j.cell.2004.12.024 (2005).

11   Picard, D. *et al.* Reduced levels of hsp90 compromise steroid receptor action in vivo. *Nature* **348**, 166-168, doi:10.1038/348166a0 (1990).

12   Morishima, Y., Murphy, P. J., Li, D. P., Sanchez, E. R. & Pratt, W. B. Stepwise assembly of a glucocorticoid receptor.hsp90 heterocomplex resolves two sequential ATP-dependent events involving first hsp70 and then hsp90 in opening of the steroid binding pocket. *J Biol Chem* **275**, 18054-18060, doi:10.1074/jbc.M000434200 (2000).

13   Smith, D. F. & Toft, D. O. Minireview: the intersection of steroid receptors with molecular chaperones: observations and questions. *Mol Endocrinol* **22**, 2229-2240, doi:10.1210/me.2008-0089 (2008).

14   Nathan, D. F. & Lindquist, S. Mutational analysis of Hsp90 function: interactions with a steroid receptor and a protein kinase. *Mol Cell Biol* **15**, 3917-3925, doi:10.1128/mcb.15.7.3917 (1995).

15   Weikum, E. R., Knuesel, M. T., Ortlund, E. A. & Yamamoto, K. R. Glucocorticoid receptor control of transcription: precision and plasticity via allostery. doi:10.1038/nrm.2016.152 (2017).

16   Pirkl, F. & Buchner, J. Functional analysis of the hsp90-associated human peptidyl prolyl Cis/Trans isomerases FKBP51, FKBP52 and cyp40. **308**, 795-806, doi:10.1006/jmbi.2001.4595 (2001).

484 17 Sinars, C. R. *et al.* Structure of the large FK506-binding protein FKBP51, an Hsp90-
485   binding protein and a component of steroid receptor complexes. *Proc Natl Acad Sci U S*
486   *A* **100**, 868-873, doi:10.1073/pnas.0231020100 (2003).
487 18 Wu, B. *et al.* 3D structure of human FK506-binding protein 52: implications for the
488   assembly of the glucocorticoid receptor/Hsp90/immunophilin heterocomplex. *Proc Natl*
489   *Acad Sci U S A* **101**, 8348-8353, doi:10.1073/pnas.0305969101 (2004).
490 19 Kumar, R., Moche, M., Winblad, B. & Pavlov, P. F. Combined x-ray crystallography and
491   computational modeling approach to investigate the Hsp90 C-terminal peptide binding
492   to FKBP51. *Sci Rep* **7**, 14288, doi:10.1038/s41598-017-14731-z (2017).
493 20 Lee, K. *et al.* The structure of an Hsp90-immunophilin complex reveals cochaperone
494   recognition of the client maturation state. *Mol Cell* **81**, 3496-3508 e3495,
495   doi:10.1016/j.molcel.2021.07.023 (2021).
496 21 Cheung-Flynn, J., Roberts, P. J., Riggs, D. L. & Smith, D. F. C-terminal sequences outside
497   the tetratricopeptide repeat domain of FKBP51 and FKBP52 cause differential binding to
498   Hsp90. *J Biol Chem* **278**, 17388-17394, doi:10.1074/jbc.M300955200 (2003).
499 22 Galigniana, M. D., Radanyi, C., Renoir, J. M., Housley, P. R. & Pratt, W. B. Evidence that
500   the peptidylprolyl isomerase domain of the hsp90-binding immunophilin FKBP52 is
501   involved in both dynein interaction and glucocorticoid receptor movement to the
502   nucleus. *J Biol Chem* **276**, 14884-14889, doi:10.1074/jbc.M010809200 (2001).
503 23 Riggs, D. L. *et al.* The Hsp90-binding peptidylprolyl isomerase FKBP52 potentiates
504   glucocorticoid signaling in vivo. *The EMBO Journal* **22**, 1158-1167,
505   doi:10.1093/emboj/cdg108 (2003).
506 24 Wochnik, G. M. *et al.* FK506-binding Proteins 51 and 52 Differentially Regulate Dynein
507   Interaction and Nuclear Translocation of the Glucocorticoid Receptor in Mammalian
508   Cells. *Journal of Biological Chemistry* **280**, 4609-4616, doi:10.1074/jbc.m407498200
509   (2005).
510 25 Tatro, E. T., Everall, I. P., Kaul, M. & Achim, C. L. Modulation of glucocorticoid receptor
511   nuclear translocation in neurons by immunophilins FKBP51 and FKBP52: Implications for
512   major depressive disorder. *Brain Research* **1286**, 1-12,
513   doi:10.1016/j.brainres.2009.06.036 (2009).
514 26 Echeverría, P. C. *et al.* Nuclear import of the glucocorticoid receptor-hsp90 complex
515   through the nuclear pore complex is mediated by its interaction with Nup62 and
516   importin beta. *Molecular and cellular biology* **29**, 4788-4797, doi:10.1128/MCB.00649-
517   09 (2009).
518 27 Denny, W. B., Valentine, D. L., Reynolds, P. D., Smith, D. F. & Scammell, J. G. Squirrel
519   monkey immunophilin FKBP51 is a potent inhibitor of glucocorticoid receptor binding.
520   *Endocrinology* **141**, 4107-4113, doi:10.1210/endo.141.11.7785 (2000).
521 28 Davies, T. H., Ning, Y. M. & Sanchez, E. R. Differential control of glucocorticoid receptor
522   hormone-binding function by tetratricopeptide repeat (TPR) proteins and the
523   immunosuppressive ligand FK506. *Biochemistry* **44**, 2030-2038, doi:10.1021/bi048503v
524   (2005).
525 29 Riggs, D. L. *et al.* Noncatalytic role of the FKBP52 peptidyl-prolyl isomerase domain in
526   the regulation of steroid hormone signaling. *Mol Cell Biol* **27**, 8658-8669,
527   doi:10.1128/MCB.00985-07 (2007).

30   Wolf, I. M. *et al.* Targeted ablation reveals a novel role of FKBP52 in gene-specific regulation of glucocorticoid receptor transcriptional activity. *J Steroid Biochem Mol Biol* **113**, 36-45, doi:10.1016/j.jsbmb.2008.11.006 (2009).

31   Hinds, T. D., Stechschulte, L. A., Elkhairi, F. & Sanchez, E. R. Analysis of FK506, timcodar (VX-853) and FKBP51 and FKBP52 chaperones in control of glucocorticoid receptor activity and phosphorylation. *Pharmacol Res Perspect* **2**, e00076, doi:10.1002/prp2.76 (2014).

32   Vandevyver, S., Dejager, L. & Libert, C. On the trail of the glucocorticoid receptor: into the nucleus and back. *Traffic* **13**, 364-374, doi:10.1111/j.1600-0854.2011.01288.x (2012).

33   Kolos, J. M., Voll, A. M., Bauder, M. & Hausch, F. FKBP Ligands-Where We Are and Where to Go? *Front Pharmacol* **9**, 1425, doi:10.3389/fphar.2018.01425 (2018).

34   Gaali, S. *et al.* Selective inhibitors of the FK506-binding protein 51 by induced fit. *Nat Chem Biol* **11**, 33-37, doi:10.1038/nchembio.1699 (2015).

35   Guy, N. C., Garcia, Y. A. & Cox, M. B. Therapeutic Targeting of the FKBP52 Co-Chaperone in Steroid Hormone Receptor-Regulated Physiology and Disease. *Curr Mol Pharmacol* **9**, 109-125, doi:10.2174/1874467208666150519114115 (2015).

36   Feng, X., Pomplun, S. & Hausch, F. Recent Progress in FKBP Ligand Development. *Curr Mol Pharmacol* **9**, 27-36, doi:10.2174/1874467208666150519113313 (2015).

37   Sabbagh, J. J. *et al.* Targeting the FKBP51/GR/Hsp90 Complex to Identify Functionally Relevant Treatments for Depression and PTSD. *ACS Chem Biol* **13**, 2288-2299, doi:10.1021/acschembio.8b00454 (2018).

38   Bauder, M. *et al.* Structure-Based Design of High-Affinity Macrocyclic FKBP51 Inhibitors. *J Med Chem* **64**, 3320-3349, doi:10.1021/acs.jmedchem.0c02195 (2021).

39   Estebanez-Perpina, E. *et al.* A surface on the androgen receptor that allosterically regulates coactivator binding. *Proc Natl Acad Sci U S A* **104**, 16074-16079, doi:10.1073/pnas.0708036104 (2007).

40   Blundell, K. L., Pal, M., Roe, S. M., Pearl, L. H. & Prodromou, C. The structure of FKBP38 in complex with the MEEVD tetratricopeptide binding-motif of Hsp90. *PLoS One* **12**, e0173543, doi:10.1371/journal.pone.0173543 (2017).

41   Fuller, P. J., Smith, B. J. & Rogerson, F. M. Cortisol resistance in the New World revisited. *Trends Endocrinol Metab* **15**, 296-299, doi:10.1016/j.tem.2004.07.001 (2004).

42   Cluning, C. *et al.* The helix 1-3 loop in the glucocorticoid receptor LBD is a regulatory element for FKBP cochaperones. *Mol Endocrinol* **27**, 1020-1035, doi:10.1210/me.2012-1023 (2013).

43   Bracher, A. *et al.* Crystal structures of the free and ligand-bound FK1-FK2 domain segment of FKBP52 reveal a flexible inter-domain hinge. *J Mol Biol* **425**, 4134-4144, doi:10.1016/j.jmb.2013.07.041 (2013).

44   Yu, K. *et al.* qPTM: an updated database for PTM dynamics in human, mouse, rat and yeast. *Nucleic Acids Res*, doi:10.1093/nar/gkac820 (2022).

45   Bledsoe, R. K. *et al.* Crystal Structure of the Glucocorticoid Receptor Ligand Binding Domain Reveals a Novel Mode of Receptor Dimerization and Coactivator Recognition. **110**, 93-105, doi:10.1016/s0092-8674(02)00817-6 (2002).

571 46 Gruszczyk, J. *et al.* Cryo-EM structure of the agonist-bound Hsp90-XAP2-AHR cytosolic
572   complex. *Nat Commun* **13**, 7010, doi:10.1038/s41467-022-34773-w (2022).

573 47 Ebong, I.-O., Beilsten-Edmands, V., Patel, N. A., Morgner, N. & Robinson, C. V. The
574   interchange of immunophilins leads to parallel pathways and different intermediates in
575   the assembly of Hsp90 glucocorticoid receptor complexes. **2**, 16002,
576   doi:10.1038/celldisc.2016.2 (2016).

577 48 Ali, M. M. U. *et al.* Crystal structure of an Hsp90–nucleotide–p23/Sba1 closed chaperone
578   complex. *Nature* **440**, 1013-1017, doi:10.1038/nature04716 (2006).

579 49 Bose, S., Weikl, T., Bugl, H. & Buchner, J. Chaperone function of Hsp90-associated
580   proteins. *Science* **274**, 1715-1717, doi:10.1126/science.274.5293.1715 (1996).

581 50 Kaziales, A., Barkovits, K., Marcus, K. & Richter, K. Glucocorticoid receptor complexes
582   form cooperatively with the Hsp90 co-chaperones Pp5 and FKBPs. *Sci Rep* **10**, 10733,
583   doi:10.1038/s41598-020-67645-8 (2020).

584 51 Verba, K. A. *et al.* Atomic structure of Hsp90-Cdc37-Cdk4 reveals that Hsp90 traps and
585   stabilizes an unfolded kinase. *Science* **352**, 1542-1547, doi:10.1126/science.aaf5023
586   (2016).

587 52 Reynolds, P. D., Ruan, Y., Smith, D. F. & Scammell, J. G. Glucocorticoid Resistance in the
588   Squirrel Monkey Is Associated with Overexpression of the Immunophilin FKBP51 1. **84**,
589   663-669, doi:10.1210/jcem.84.2.5429 (1999).

590 53 Draxler, S. W. *et al.* Hybrid Screening Approach for Very Small Fragments: X-ray and
591   Computational Screening on FKBP51. *Journal of Medicinal Chemistry* **63**, 5856-5864,
592   doi:10.1021/acs.jmedchem.0c00120 (2020).

593 54 Oroz, J. *et al.* Structure and pro-toxic mechanism of the human Hsp90/PPIase/Tau
594   complex. *Nature Communications* **9**, doi:10.1038/s41467-018-06880-0 (2018).

595 55 Maeda, K. *et al.* FKBP51 and FKBP52 regulate androgen receptor dimerization and
596   proliferation in prostate cancer cells. *Mol Oncol* **16**, 940-956, doi:10.1002/1878-
597   0261.13030 (2022).

598 56 Jaime-Garza, M. *et al.* Hsp90 provides a platform for kinase dephosphorylation by PP5.
599   *bioRxiv* (2022).

600 57 Savory, J. G. A. *et al.* Discrimination between NL1- and NL2-Mediated Nuclear
601   Localization of the Glucocorticoid Receptor. **19**, 1025-1037, doi:10.1128/mcb.19.2.1025
602   (1999).

603 58 Pratt, W. B., Galigniana, M. D., Harrell, J. M. & DeFranco, D. B. Role of hsp90 and the
604   hsp90-binding immunophilins in signalling protein movement. *Cell Signal* **16**, 857-872,
605   doi:10.1016/j.cellsig.2004.02.004 (2004).

606 59 Sivils, J. C., Storer, C. L., Galigniana, M. D. & Cox, M. B. Regulation of steroid hormone
607   receptor function by the 52-kDa FK506-binding protein (FKBP52). *Curr Opin Pharmacol*
608   **11**, 314-319, doi:10.1016/j.coph.2011.03.010 (2011).

609 60 Rein, T. Peptidylprolylisomerases, Protein Folders, or Scaffolders? The Example of
610   FKBP51 and FKBP52. *Bioessays* **42**, e1900250, doi:10.1002/bies.201900250 (2020).

611 61 Mustafi, S. M., LeMaster, D. M. & Hernandez, G. Differential conformational dynamics in
612   the closely homologous FK506-binding domains of FKBP51 and FKBP52. *Biochem J* **461**,
613   115-123, doi:10.1042/BJ20140232 (2014).

614   62   Galigniana, M. D., Echeverria, P. C., Erlejman, A. G. & Piwien-Pilipuk, G. Role of
615   molecular chaperones and TPR-domain proteins in the cytoplasmic transport of steroid
616   receptors and their passage through the nuclear pore. *Nucleus* **1**, 299-308,
617   doi:10.4161/nucl.1.4.11743 (2010).
618   63   Baughman, G., Wiederrecht, G. J., Chang, F., Martin, M. M. & Bourgeois, S. Tissue
619   distribution and abundance of human FKBP51, and FK506-binding protein that can
620   mediate calcineurin inhibition. *Biochem Biophys Res Commun* **232**, 437-443,
621   doi:10.1006/bbrc.1997.6307 (1997).
622   64   Jaaskelainen, T., Makkonen, H. & Palvimo, J. J. Steroid up-regulation of FKBP51 and its
623   role in hormone signaling. *Curr Opin Pharmacol* **11**, 326-331,
624   doi:10.1016/j.coph.2011.04.006 (2011).
625   65   Zannas, A. S. & Binder, E. B. Gene-environment interactions at the FKBP5 locus: sensitive
626   periods, mechanisms and pleiotropism. *Genes Brain Behav* **13**, 25-37,
627   doi:10.1111/gbb.12104 (2014).
628   66   Zannas, A. S., Wiechmann, T., Gassen, N. C. & Binder, E. B. Gene-Stress-Epigenetic
629   Regulation of FKBP5: Clinical and Translational Implications. *Neuropsychopharmacology*
630   **41**, 261-274, doi:10.1038/npp.2015.235 (2016).
631   67   Cheung, J. & Smith, D. F. Molecular chaperone interactions with steroid receptors: an
632   update. *Mol Endocrinol* **14**, 939-946, doi:10.1210/mend.14.7.0489 (2000).
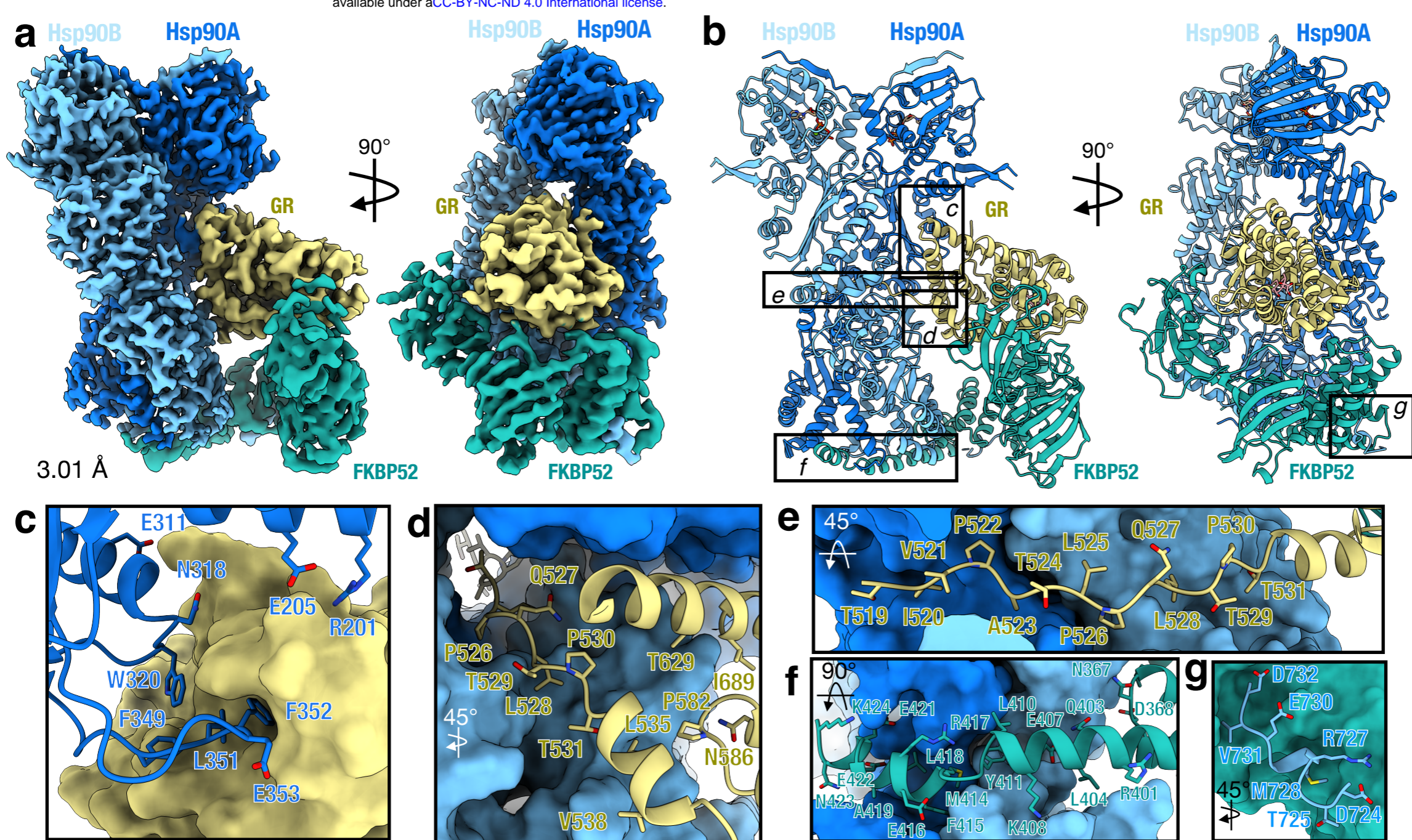633
634

Figure 1 | Architecture of the GR:Hsp90:FKBP52 complex

a, Composite cryo-EM map of the GR:Hsp90:FKBP52 complex. Hsp90A (dark blue), Hsp90B (light blue), GR (yellow), FKBP52 (teal). Color scheme is maintained throughout. **b,** Atomic model in cartoon representation with boxes corresponding to the interfaces shown in detail in **b-g**. **c,** Interface 1 of the Hsp90:GR interaction, depicting the Hsp90A Src loop (Hsp90A$^{345-360}$) interacting with the GR hydrophobic patch. GR is in surface representation. **d,** Interface 2 of the Hsp90:GR interaction, depicting GR$_{Helix 1}$ (GR$^{532-539}$) packing against the entrance to the Hsp90 lumen. Hsp90A/B are in surface representation. **e,** Interface 3 of the Hsp90:GR interaction, depicting GR$_{pre-Helix 1}$ (GR$^{519-531}$) threading through the Hsp90 lumen. Hsp90A/B are in surface representation. **f,** Interface 1 of the Hsp90:FKBP52 interaction, depicting FKBP52 TPR H7e (FKBP52$^{387-424}$) interacting with the Hsp90A/B CTD dimer interface. Hsp90A/B are in surface representation. **g,** Interface 2 of the Hsp90:FKBP52 interaction, depicting the Hsp90B MEEVD motif (Hsp90B$^{700-706}$) binding in the helical bundle of the FKBP52 TPR domain. FKBP52 is in surface representation.
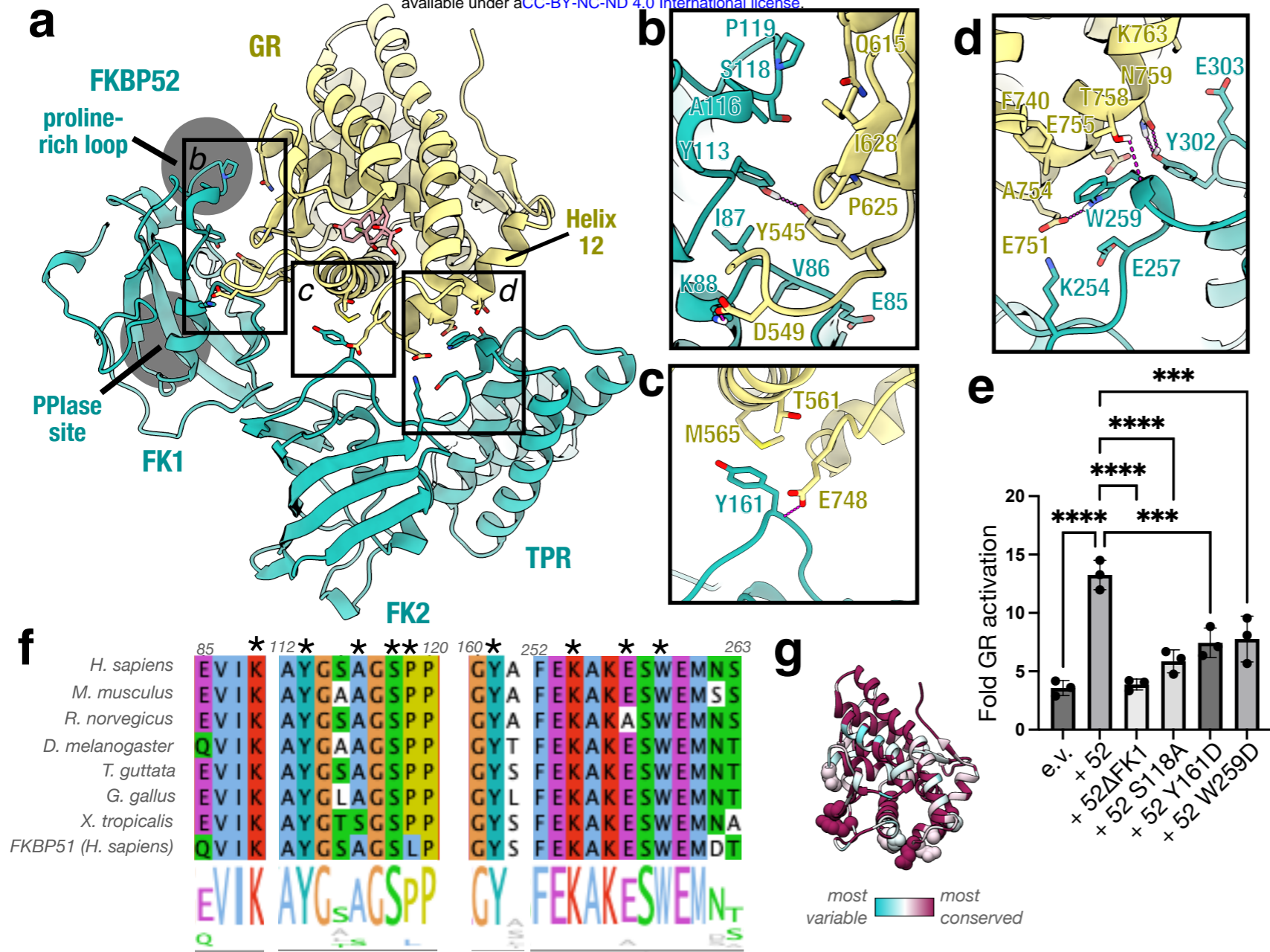
Figure 2 | The GR:FKBP52 interaction and functional significance

a, Atomic model depicting the three interfaces between GR (yellow) and FKBP52 (teal) in the GR:Hsp90:FKBP52 complex. The FKBP52 proline-rich loop and PPIase site catalytic site are highlighted in gray. **b,** Interface 1 between GR (yellow) and the FKBP52 FK1 domain (teal), showing interacting side chains and hydrogen bonds (dashed pink lines). **c,** Interface 2 between GR (yellow) and the FKBP52 FK2 domain (teal), showing interacting side chains and hydrogen bonds (dashed pink lines). **d,** Interface 3 between GR (yellow) and the FKBP52 FK2-TPR linker (teal), showing interacting side chains and hydrogen bonds (dashed pink lines). **e,** GR activation assay in wild-type yeast strain JJ762 expressing FKBP52 ("52") or FKBP52 mutants. The fold increase in GR activities compared to the empty vector (e.v.) control are shown (mean±SD). n=3 biologically independent samples per condition. Significance was evaluated using a one-way ANOVA ($F_{(6,14)} = 67.82$; $p < 0.0001$) with *post-hoc* Dunnett's multiple comparisons test (n.s. $P \geq 0.05$; * $P \leq 0.05$; ** $P \leq 0.01$; *** $P \leq 0.001$). P-values: p(e.v. vs. 52) < 0.0001, p(52 vs. 52ΔFK1) < 0.0001, p(52 vs. 52 S118A) < 0.0001, p(52 vs. 52 Y161D) = 0.0001, p(52 vs. 52 W259D) = 0.0002. **f,** Sequence alignment of eukaryotic FKBP52 showing conserved residues involved in the GR:FKBP52 interaction (denoted by a black asterisk). The bottom aligned sequence is human FKBP51. The alignment is colored according to the ClustalW convention. **g,** GR protein sequence conservation mapped onto the GR atomic model from the GR:Hsp90:FKBP52 complex. Residue conservation is depicted from most variable (cyan) to most conserved residues (maroon).
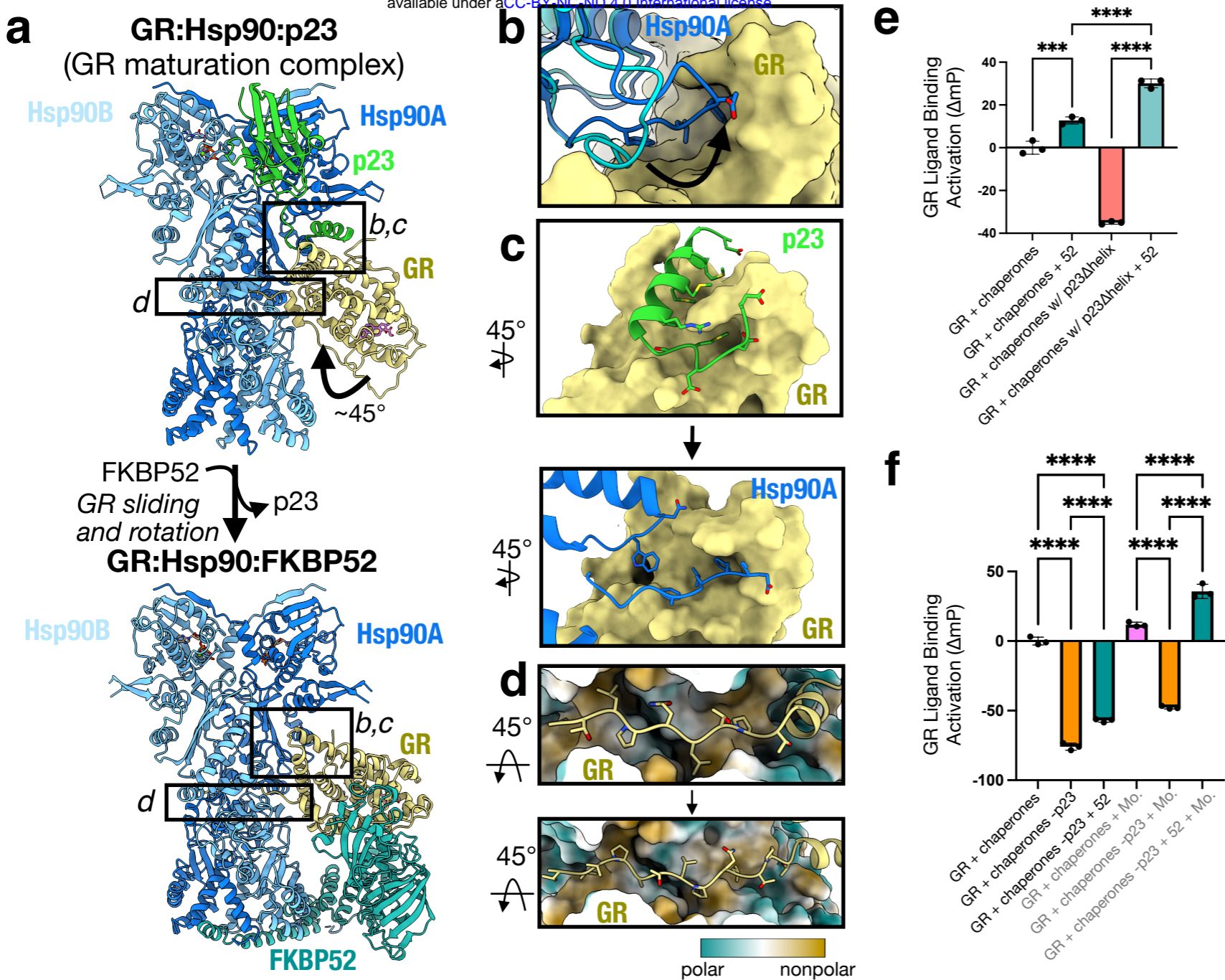
Figure 3 | FKBP52 competes with p23 to bind GR:Hsp90

a, Atomic model of the GR-maturation complex (top) and the GR:Hsp90:FKBP52 complex (bottom) with boxes corresponding to the interfaces shown in detail in **b-d**. FKBP52 competes off p23 and re-positions GR at an approximately 45° rotated position. Hsp90A (dark blue), Hsp90B (light blue), GR (yellow), p23 (green), FKBP52 (teal). **b,** Position of the Hsp90A Src loop in the GR-maturation complex (Hsp90A, cyan) versus the GR:Hsp90:FKBP52 complex (Hsp90A, dark blue). The Hsp90A Src loop flips up in the GR:Hsp90:FKBP52 complex to interact with the hydrophobic patch on the rotated GR (yellow, surface representation). Hsp90A Src loop residues interacting with the GR hydrophobic patch are shown. **c,** Interface between the p23 tail-helix (green) and the GR hydrophobic patch (yellow, surface representation) in the GR-maturation complex (top). The p23 tail-helix is replaced by the Hsp90A Src loop (dark blue) in the GR:Hsp90:FKBP52 complex (bottom), which flip up to interact with the GR hydrophobic patch (yellow, surface representation). Interacting side chains are shown. **d,** Interaction between the $GR_{pre-Helix\ 1}$ ($GR^{523-531}$) threading through the Hsp90 lumen in the GR-maturation complex (top) versus the $GR_{pre-Helix\ 1}$ ($GR^{519-531}$) threading through the Hsp90 lumen in the GR:Hsp90:FKBP52 complex (bottom). Hsp90A/B are in surface representation colored by hydrophobicity. The $GR_{pre-Helix\ 1}$ region translocates through the Hsp90 lumen by 2 residues in the transition from the GR-maturation complex to the GR:Hsp90:FKBP52 complex. Two hydrophobic residues on $GR_{pre-Helix\ 1}$ ($GR^{L525,L528}$ or $GR^{P522,P526}$) remain bound in the Hsp90 lumen hydrophobic pockets in both complexes. **e,** Equilibrium binding of 10nM fluorescent dexamethasone to 100nM GR DBD-LBD with chaperones and FKBP52 ("52"). "Chaperones"= 15uM Hsp70, Hsp90, Hop, and p23 or p23Δhelix, 2uM Ydj1 and Bag-1. Significance was evaluated using a one-way ANOVA ($F_{(3,8)} = 541.2$; $p < 0.0001$) with *post-hoc* Šídák's test (n.s. $P \geq 0.05$; * $P \leq 0.05$; ** $P \leq 0.01$; *** $P \leq 0.001$; **** $P \leq 0.0001$). P-values: p(Chaperones vs. Chaperones) + 52 = 0.0002, p(Chaperones + 52 vs. Chaperones w/ p23Δhelix + 52) < 0.0001, p(Chaperones w/ p23Δhelix vs. Chaperones w/ p23Δhelix + 52) < 0.0001. **f,** Equilibrium binding of 10nM fluorescent dexamethasone to 100nM GR DBD-LBD with chaperones, FKBP52 ("52"), and sodium molybdate ("Mo"). "Chaperones"= 15uM Hsp70, Hsp90, Hop, and p23, 2uM Ydj1 and Bag-1. Significance was evaluated using a one-way ANOVA ($F_{(5,12)} = 761.5$; $p < 0.0001$) with *post-hoc* Šídák's test (n.s. $P \geq 0.05$; * $P \leq 0.05$; ** $P \leq 0.01$; *** $P \leq 0.001$; **** $P \leq 0.0001$). P-values < 0.0001 for each comparison.
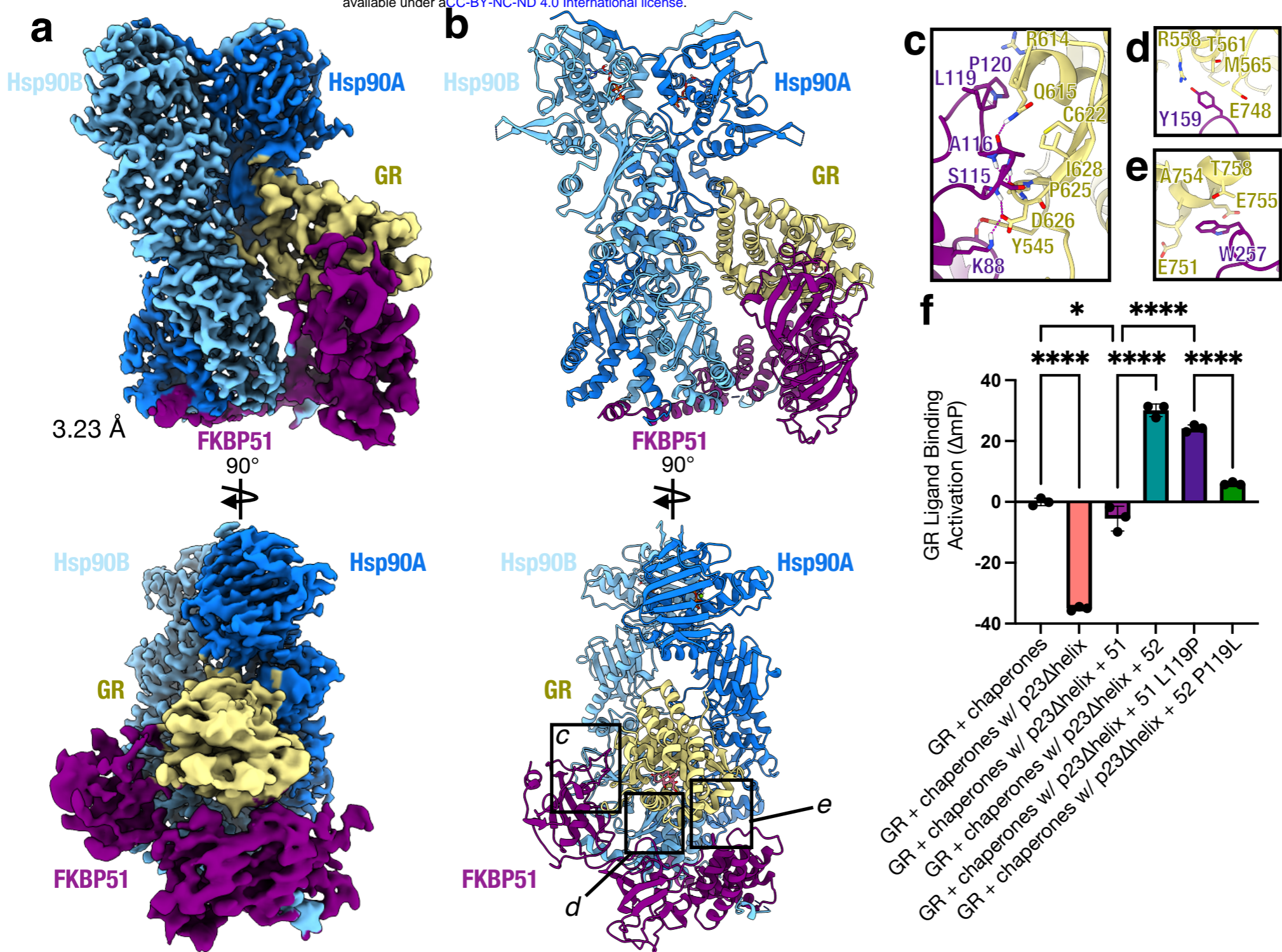
Figure 4 | Architecture of the GR:Hsp90:FKBP51 complex

a, Composite cryo-EM map of the GR:Hsp90:FKBP51 complex. Hsp90A (dark blue), Hsp90B (light blue), GR (yellow), FKBP51 (purple). Color scheme is maintained throughout. **b,** Atomic model in cartoon representation with boxes corresponding to the interfaces shown in detail in **c-e**. **c,** Interface 1 between GR (yellow) and the FKBP51 FK1 domain (purple), showing interacting side chains and hydrogen bonds (dashed pink lines). **d,** Interface 2 between GR (yellow) and the FKBP51 FK2 domain (purple), showing interacting side chains and hydrogen bonds (dashed pink lines). **e,** Interface 3 between GR (yellow) and the FKBP51 FK2-TPR linker (yellow), showing interacting side chains and hydrogen bonds (dashed pink lines). **f,** Equilibrium binding of 10nM fluorescent dexamethasone to 100nM GR DBD-LBD with chaperones, FKBP51 ("51"), FKBP52 ("52"), or mutants. "Chaperones"= 15uM Hsp70, Hsp90, Hop, and p23 or p23Δhelix, 2uM Ydj1 and Bag-1. Significance was evaluated using a one-way ANOVA ($F_{(5,12)}$ = 404.1; $p < 0.0001$) with *post-hoc* Šídák's test (n.s. $P \geq 0.05$; * $P \leq 0.05$; ** $P \leq 0.01$; *** $P \leq 0.001$; **** $P \leq 0.0001$). See **Methods** for p-values.
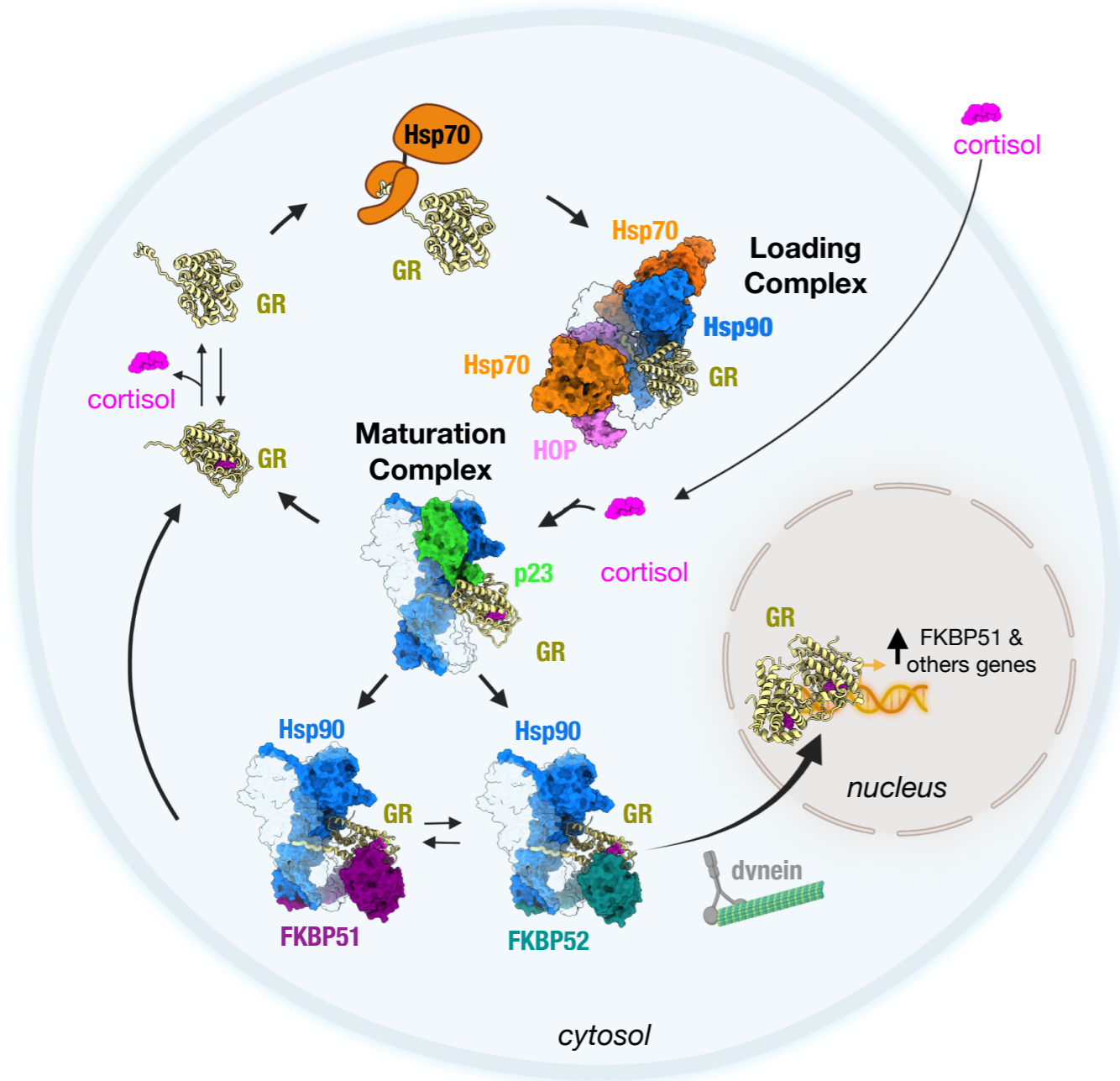
Figure 5 | Mechanism of GR regulation by FKBP51 and FKBP52 in the GR chaperone cycle *in vivo*
Schematic of the GR chaperone cycle in the cell. Starting on the top left, GR (yellow, cartoon representation) is in dynamic equilibrium between cortisol-bound and unbound (apo) states. Hsp70 (orange) binds GR and locally unfolds GR to inhibit cortisol-binding, stabilizing GR in a partially unfolded, apo state. Hsp70 transfers the partially unfolded GR to Hsp90 (light and dark blue):Hop (pink) to form the GR-loading complex (Wang et al. 2022), in which GR is stabilized in a partially unfolded, apo state with the cortisol-binding pocket accessible. Cortisol (pink), which enters the cell through diffusion, binds to GR during the transition from the GR-loading complex to the GR-maturation complex when Hsp90 refolds the GR to a native conformation, sealing the cortisol-binding pocket through the refolding of the GR Helix 1 region (Noddings et al. 2022). In the GR-maturation complex, the cortisol-bound, folded GR is stabilized by Hsp90 and p23 (green), and is protected from Hsp70 re-binding. Depending on the relative concentrations of the FKBPs, either FKBP51 (purple) or FKBP52 (teal) can bind the GR:Hsp90:p23 complex, competing off p23, and stabilizing the rotated position of GR. FKBP51 sequesters GR:Hsp90 in the cytosol until ATP hydrolysis on Hsp90 allows release of GR back to the chaperone cycle. In contrast, FKBP52 promotes rapid nuclear translocation of GR:Hsp90 by acting as an adapter to the dynein/dynactin motor complex. Once in the nucleus, the cortisol-bound GR can dimerize, nucleate the assembly of transcriptional regulatory complexes, and activate the transcription of thousands of genes, including the gene for FKBP51 (*FKBP5*), leading to a negative feedback loop that regulates GR activity in the cell. The GR chaperone cycle also occurs in the absence of ligand and evidence supports preferential binding of FKBP51 over FKBP52 to apo GR:Hsp90 complexes, insuring the apo (inactivated) GR is not improperly translocated to the nucleus to regulate transcription.